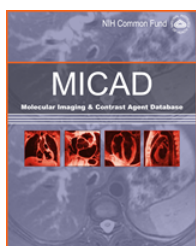


NLM Citation: Shan L. ^{111}In -Labeled 1,4,7,10-tetraazacyclododecane-1,4,7,10-tetracetic acid-Glu{PEG₄-Glu[cyclo(Lys-Arg-Gly-Asp-D-Phe)]-cyclo(Lys-Arg-Gly-Asp-D-Phe)}-{PEG₄-Glu[cyclo(Lys-Arg-Gly-Asp-D-Phe)]-cyclo(Lys-Arg-Gly-Asp-D-Phe)} (PEG₄ = 15 amino-4,7,10,13-tetraoxapentadecanoic acid). 2012 Feb 23 [Updated 2012 Mar 22]. In: Molecular Imaging and Contrast Agent Database (MICAD) [Internet]. Bethesda (MD): National Center for Biotechnology Information (US); 2004-2013.

Bookshelf URL: <https://www.ncbi.nlm.nih.gov/books/>



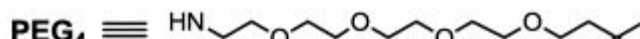
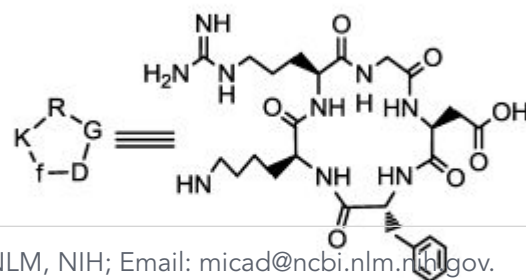
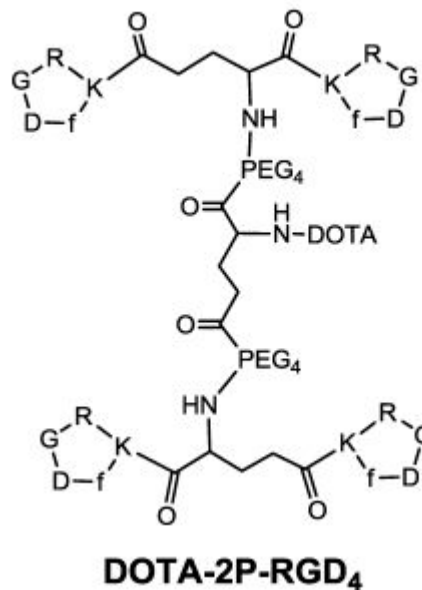
^{111}In -Labeled 1,4,7,10-tetraazacyclododecane-1,4,7,10-tetracetic acid-Glu{PEG₄-Glu[cyclo(Lys-Arg-Gly-Asp-D-Phe)]-cyclo(Lys-Arg-Gly-Asp-D-Phe)}-{PEG₄-Glu[cyclo(Lys-Arg-Gly-Asp-D-Phe)]-cyclo(Lys-Arg-Gly-Asp-D-Phe)} (PEG₄ = 15 amino-4,7,10,13-tetraoxapentadecanoic acid)

^{111}In (DOTA-2P-RGD₄)

Liang Shan, PhD¹

Created: February 23, 2012; Updated: March 22, 2012.

Chemical name:	^{111}In -Labeled 1,4,7,10-tetraazacyclododecane-1,4,7,10-tetracetic acid-Glu{PEG ₄ -Glu[cyclo(Lys-Arg-Gly-Asp-D-Phe)]-cyclo(Lys-Arg-Gly-Asp-D-Phe)}-{PEG ₄ -Glu[cyclo(Lys-Arg-Gly-Asp-D-Phe)]-cyclo(Lys-Arg-Gly-Asp-D-Phe)} (PEG ₄ = 15 amino-4,7,10,13-tetraoxapentadecanoic acid)
Abbreviated name:	^{111}In (DOTA-2P-RGD ₄)
Synonym:	^{111}In -DOTA-E{PEG ₄ -E[c(RGDfK)] ₂ } ₂
Agent Category:	Peptides
Target:	Integrin alphavbeta3 ($\alpha_v\beta_3$)
Target Category:	Receptors
Method of detection:	Single-photon emission computed tomography (SPECT) or planar imaging
Source of signal / contrast:	^{111}In
Activation:	No



Author Affiliation: 1 National Center for Biotechnology Information, NLM, NIH; Email: micad@ncbi.nlm.nih.gov.

Table continued from previous page.

Studies:	<ul style="list-style-type: none"> • <i>In vitro</i> • Rodents 	Structures of $^{111}\text{In}(\text{DOTA-2P-RGD}_4)$ by Shi et al. (1).
-----------------	--	--

Background

[PubMed]

The ^{111}In -labeled 1,4,7,10-tetraazacyclododecane-1,4,7,10-tetracetic acid (DOTA)-Glu{PEG₄-Glu[cyclo(Lys-Arg-Gly-Asp-D-Phe)]-cyclo(Lys-Arg-Gly-Asp-D-Phe)}-cyclo(Lys-Arg-Gly-Asp-D-Phe)}-cyclo(Lys-Arg-Gly-Asp-D-Phe)} (PEG₄ = 15 amino-4,7,10,13-tetraoxapentadecanoic acid), abbreviated as $^{111}\text{In}(\text{DOTA-2P-RGD}_4)$ or $^{111}\text{In-DOTA-E}\{\text{PEG}_4\text{-E}[\text{c}(\text{RGDfK})]_2\}_2$, was synthesized by Shi et al. as an agent for molecular imaging of tumor angiogenesis by targeting integrin $\alpha_v\beta_3$ (1). Here, P = PEG₄ = 15 amino-4,7,10,13-tetraoxapentadecanoic acid = a linker between two c(RGDfK) motifs; c(RGDfK) = cyclo(Lys-Arg-Gly-Asp-D-Phe); RGD₄ = four motifs of c(RGDfK); and E = Glu.

Integrin $\alpha_v\beta_3$ is a receptor that is overexpressed on the activated endothelial cells of tumors (2). Because the integrin $\alpha_v\beta_3$ binds with extracellular matrix proteins (e.g., vitronectin, fibronectin) through the exposed Arg-Gly-Asp tripeptide sequence, RGD-containing peptides have been intensively studied in the past decade as a vector for imaging $\alpha_v\beta_3$ expression (3, 4). Although significant progress has been made, improving the binding affinity and pharmacokinetics of RGD peptides remains the major consideration in the design of agents, and various strategies have been developed for this improvement, such as the use of RGD multimers, the introduction of sugar amino acids or D-amino acids into the RGD peptides, and the conjugation of the RGD peptides with chelators or polyethylene glycol (PEG) chains (5, 6).

The concept of multimerization has been developed to address the question of multimeric binding by "poly-potent" ligands. Multimers are formed by bridging monomeric units through linker(s) (2, 7). The multimer effect has been demonstrated in different studies, showing that the binding affinity of RGD peptides increases in the order of monomer < dimer < tetramer < octamer. For example, the cyclo(-RGDfE)-monomer, dimer, and tetramer containing heptaethylene glycol spacer units have been shown to exhibit $\alpha_v\beta_3$ -binding affinities that increase by a factor of ten with each duplication of binding units (8). The integrin affinity of the DOTA-RGD octamer has been shown to be three-fold higher than that of the DOTA-RGD tetramer (7).

Recently, investigators from Purdue University suggested a concept of "bivalency" for the $\alpha_v\beta_3$ -binding affinity of RGD-containing peptides (1, 6, 9). The main point of this concept is that the multimeric cyclic RGD peptides are likely bivalent rather than multivalent in binding to integrin $\alpha_v\beta_3$, and enough distance between two RGD motifs is the key for bivalency (1, 5, 10). For example, the dimeric peptide E[c(RGDfK)]₂ (RGD₂) is monovalent, whereas the dimeric peptides PEG₄-E[PEG₄-c(RGDfK)]₂ (3P-RGD₂) and G₃-E[G₃-c(RGDfK)]₂ (3G-RGD₂) (G = G₃ = Gly-Gly-Gly linker) are bivalent because of the increased distance between the two cyclic RGD motifs for simultaneous integrin $\alpha_v\beta_3$ binding in the latter two peptides (5). The cyclic RGD tetramers, such as DOTA-RGD₄ and DOTA-E{G₃-E[G₃-c(RGDfK)]₂}_2 (DOTA-6G-RGD₄), are also likely bivalent in binding to integrin $\alpha_v\beta_3$ even though they contain four identical RGD motifs (5, 10). Studies with three other tetramers (DOTA-2P-RGD₄, DOTA-2P4G-RGD₄, and DOTA-6P-RGD₄) have further shown that the three tetramers are not tetravalent, although the tetramers exhibited a higher binding affinity to $\alpha_v\beta_3$ than monomers and dimers, and the "locally enriched" RGD concentration has been considered to contribute to the higher binding affinity (1, 6). The linkers between RGD motifs may have a significant impact on the integrin $\alpha_v\beta_3$ -targeting capability, biodistribution, excretion kinetics, and metabolic stability of cyclic RGD peptides (1, 11, 12).

This chapter summarizes the data obtained with $^{111}\text{In}(\text{DOTA-2P-RGD}_4)$. Other chapters summarize the data obtained with $^{111}\text{In}(\text{DOTA-6P-RGD}_4)$ and $^{111}\text{In}(\text{DOTA-2P4G-RGD}_4)$, respectively.

Related Resource Links:

The nucleotide and protein sequences of integrin $\alpha_v\beta_3$

Integrin $\alpha_v\beta_3$ -related imaging agents in MICAD

Articles of integrin $\alpha_v\beta_3$ in Online Mendelian Inheritance in Man

Integrin $\alpha_v\beta_3$ -related clinical trials in ClinTrials.gov

Synthesis

[PubMed]

The RGD-containing peptides were all custom-made, including P-RGD, P2G-RGD₂, 3P-RGD₂, and 3P-RGK₂ (RGK = cyclo(Arg-Gly-Lys-D-Phe-Asp)). The tetramers were synthesized by the reaction of Boc-E(OSu)₂ and their corresponding dimers (1). Conjugation of the RGD peptides with DOTA-OSu resulted in their corresponding conjugates (DOTA-P-RGD, DOTA-P-RGD₂, DOTA-3P-RGD₂, DOTA-2P-RGD₄, DOTA-2P4G-RGD₄, and DOTA-6P-RGD₄, respectively). DOTA-6P-RGK₄ was prepared using a procedure identical to that for DOTA-6P-RGD₄. DOTA-6P-RGK₄ has the identical amino acids, but its sequence is scrambled to demonstrate the RGD-specificity of DOTA-6P-RGD₄. The identities for all RGD conjugates were confirmed, and their purities were all >95% before being used for ^{111}In labeling and determination of their integrin $\alpha_v\beta_3$ binding affinity. Table 1 lists the molecular weights and yields of each DOTA-conjugated peptide (1).

Table 1: The physicochemical characteristics of the RGD peptides.

Agents	DOTA-P-RGD	DOTA-P-RGD ₂	DOTA-3P-RGD ₂ *	DOTA-2P-RGD ₄	DOTA-2P4G-RGD ₄	DOTA-6P-RGD ₄	DOTA-6P-RGK ₄
MW	1,237.58	1,951.5	2,447.35	3,626.4	4,315.4	4,622.7	4,622.7
Yield	~40%	~41%	~30%	~56%	~64%	~43%	~68%

*The data for DOTA-3P-RGD₂ were obtained from Shi et al. (5).

All ^{111}In -labeled peptides were prepared by reacting $^{111}\text{InCl}_3$ with the respective DOTA conjugates in NH₄OAc buffer (100 mM, pH = 5.5). Radiolabeling was completed by heating the reaction mixture at 100°C for ~15 min. After purification, the radiochemical purity was >95% and the specific activity was >40 mCi/μmol (1.48 GBq/μmol) for all ^{111}In -labeled RGD peptides (1).

In Vitro Studies: Testing in Cells and Tissues

[PubMed]

The integrin binding affinity and specificity of the RGD peptides were assessed in U87MG human glioma whole cells, with ^{125}I -c(RGDyK) as the integrin-specific radioligand (1). The $\alpha_v\beta_3$ binding affinity of the peptides followed the order of DOTA-6P-RGD₄ ~ DOTA-2P4G-RGD₄ ~ DOTA-2P-RGD₄ > DOTA-P-RGD₂ > DOTA-P-RGD > RGD (IC₅₀ = 49.9) (Table 1). The binding affinity of DOTA-3P-RGD₂ was significantly higher than that of DOTA-P-RGD and DOTA-P-RGD₂ (P < 0.01). However, the investigators found that the integrin $\alpha_v\beta_3$ binding affinities of DOTA-2P-RGD₄, DOTA-2P4G-RGD₄, and DOTA-6P-RGD₄ were only marginally higher than that of DOTA-3P-RGD₂, suggesting that they might share the same bivalency in binding to the integrin $\alpha_v\beta_3$.

Shi et al. also determined the water-octanol partition coefficients and stability of the ^{111}In -labeled peptides (1). The log P values are listed in Table 2. The ^{111}In -labeled peptides remained stable for >72 h after purification in the presence of 3 mM EDTA.

Table 2: The IC_{50} and log P values of the ^{111}In -labeled cyclic RGD peptides.

Peptides	DOTA-P-RGD	DOTA-P-RGD ₂	DOTA-3P-RGD ₂	DOTA-2P-RGD ₄	DOTA-2P4G-RGD ₄	DOTA-6P-RGD ₄	DOTA-6P-RGK ₄
IC_{50} (nM)	44.3	5.0	1.5	0.5	0.2	0.3	437
Log P	-3.48	-3.22	-4.20	-3.87	-3.93	-3.68	-3.61

IC_{50} : half-maximal inhibitory concentration.

Animal Studies

Rodents

[PubMed]

Biodistribution, imaging, and metabolic studies were performed in athymic nude mice bearing U87MG human glioma xenografts in both left and right upper flanks (1).

For the biodistribution studies, each mouse was administered $\sim 3 \mu\text{Ci}$ ($\sim 0.111 \text{ MBq}$) of the agent *via* tail vein injection (1). Mice were then euthanized at 0.5, 1, 4, 24, and 72 h after injection ($n = 5$ mice/time point). The organ uptake was calculated as the percentage of injected dose per gram of organ mass (% ID/g). The tumor and intestinal uptake values of $^{111}\text{In}(\text{DOTA-2P-RGD}_4)$ were high and close to those of $^{111}\text{In}(\text{DOTA-6P-RGD}_4)$ over the 72-h period. $^{111}\text{In}(\text{DOTA-2P-RGD}_4)$ also had a rapid clearance from normal organs, such as the blood, kidneys, and liver. Therefore, the tumor/liver and tumor/kidney ratios for $^{111}\text{In}(\text{DOTA-2P-RGD}_4)$ were comparable to those obtained for $^{111}\text{In}(\text{DOTA-6P-RGD}_4)$ and $^{111}\text{In}(\text{DOTA-6G-RGD}_4)$.

Table 3: Selected biodistribution data of $^{111}\text{In}(\text{DOTA-2P-RGD}_4)$.

% ID/g	0.5 h	1 h	24 h	72 h
Blood	1.12 \pm 0.08	0.31 \pm 0.16	0.03 \pm 0.00	0.02 \pm 0.02
U87MG	12.98 \pm 5.99	10.66 \pm 2.4	6.52 \pm 3.85	2.87 \pm 1.45
Tumor/Blood	11.60 \pm 5.36	34.67 \pm 7.84	231.33 \pm 136.67	192.06 \pm 172.1
Tumor/Kidney	1.46 \pm 0.67	1.60 \pm 0.27	1.46 \pm 0.80	1.28 \pm 0.59
Tumor/Liver	6.09 \pm 2.81	4.34 \pm 1.12	4.19 \pm 1.04	4.89 \pm 1.62
Tumor/Lungs	4.06 \pm 1.88	4.31 \pm 0.96	6.76 \pm 3.99	8.94 \pm 5.37
Tumor/Muscle	13.92 \pm 6.43	11.76 \pm 3.58	16.78 \pm 9.92	25.87 \pm 15.57

No blocking experiment was performed with $^{111}\text{In}(\text{DOTA-2P-RGD}_4)$. The blocking experimental data obtained with $^{111}\text{In}(\text{DOTA-6P-RGD}_4)$ are summarized in the chapter on $^{111}\text{In}(\text{DOTA-6P-RGD}_4)$ in MICAD (1).

The imaging studies were performed after tail vein administration of $\sim 100 \mu\text{Ci}$ (3.7 MBq) $^{111}\text{In}(\text{DOTA-2P-RGD}_4)$ ($n = 3$ mice) (1). The whole-body images were acquired at 0.5, 1, 4, 24, and 72 h after injection. The tumors were clearly visualized with excellent tumor/background contrast as early as 1 h after injection. A long tumor retention time was observed, which was consistent with the biodistribution results. The time to half-maximal radioactivity in tumors was >30 h for $^{111}\text{In}(\text{DOTA-2P-RGD}_4)$, $^{111}\text{In}(\text{DOTA-2P4G-RGD}_4)$, and $^{111}\text{In}(\text{DOTA-6P-RGD}_4)$ (1).

For the metabolism studies, each mouse was given $\sim 100 \mu\text{Ci}$ (3.7 MBq) $^{111}\text{In}(\text{DOTA-6P-RGD}_4)$ *via* tail vein injection (1). The urine samples were collected at 30 min and 120 min after injection, and the feces samples were collected at 120 min. The percentage of radioactivity recovery was $>95\%$ (by γ -counting) for both urine and feces. There were very limited radioactivity accumulation in the liver and kidneys. There was little metabolism detected in the urine or feces samples over the 2-h study period for $^{111}\text{In}(\text{DOTA-2P-RGD}_4)$.

Shi et al. comparatively analyzed the biodistribution data for $^{111}\text{In}(\text{DOTA-2P-RGD}_4)$, $^{111}\text{In}(\text{DOTA-2P4G-RGD}_4)$, $^{111}\text{In}(\text{DOTA-6P-RGD}_4)$, $^{111}\text{In}(\text{DOTA-6G-RGD}_4)$, $^{111}\text{In}(\text{DOTA-3P-RGD}_2)$, $^{111}\text{In}(\text{DOTA-P-RGD}_2)$, and $^{111}\text{In}(\text{DOTA-P-RGD})$ (1). Over the first 24 h, the tumor uptake difference between the tetramers and dimers was not significant ($P > 0.05$). The tumor uptake at 72 h (% ID/g) followed the general order of $^{111}\text{In}(\text{DOTA-6P-RGD}_4)$ (3.04) $>$ $^{111}\text{In}(\text{DOTA-2P-RGD}_4)$ (2.87) \sim $^{111}\text{In}(\text{DOTA-2P4G-RGD}_4)$ (2.66) $>$ $^{111}\text{In}(\text{DOTA-3P-RGD}_2)$ (2.18), which was similar to the trend observed with integrin $\alpha_v\beta_3$ binding affinity (IC_{50} , nM) of DOTA-6P-RGD_4 (0.3 ± 0.1) \sim DOTA-2P4G-RGD_4 (0.2 ± 0.1) \sim DOTA-2P-RGD_4 (0.5 ± 0.1) $>$ DOTA-3P-RGD_2 (1.5 ± 0.2). Among the ^{111}In -labeled radiotracers, $^{111}\text{In}(\text{DOTA-6G-RGD}_4)$ had the highest uptake in the tumor and intestine at 72 h after injection. The half-life of $^{111}\text{In}(\text{DOTA-6G-RGD}_4)$ in the tumor was estimated to be 60 h. In contrast, $^{111}\text{In}(\text{DOTA-3P-RGD}_2)$ and $^{111}\text{In}(\text{DOTA-2P4G-RGD}_4)$ had low uptake in the intestine, kidneys, and liver over the 72-h period. As a result, $^{111}\text{In}(\text{DOTA-3P-RGD}_2)$ and $^{111}\text{In}(\text{DOTA-2P4G-RGD}_4)$ had tumor/kidney and tumor/liver ratios that were significantly better ($P < 0.05$) than those of $^{111}\text{In}(\text{DOTA-6G-RGD}_4)$ and $^{111}\text{In}(\text{DOTA-6P-RGD}_4)$ during that period of time. As expected, $^{111}\text{In}(\text{DOTA-P-RGD})$ had the lowest tumor uptake (3.7% ID/g and 0.7% ID/g at 0.5 h and 72 h after injection, respectively). $^{111}\text{In}(\text{DOTA-P-RGD}_2)$ had a relatively high tumor uptake (6.1 at 0.5 h after injection), but it had a significant washout from the tumor, with uptake values being 4.9, 4.8, 3.1 and 1.6% ID/g at 1, 4, 24, and 72 h after injection, respectively. The tumor uptake values follow the trend of $^{111}\text{In}(\text{DOTA-3P-RGD}_2) >$ $^{111}\text{In}(\text{DOTA-P-RGD}_2) >$ $^{111}\text{In}(\text{DOTA-P-RGD})$, which was consistent with the order of their $\alpha_v\beta_3$ binding affinities (IC_{50} value): $\text{DOTA-3P-RGD}_2 <$ $\text{DOTA-P-RGD}_2 <$ DOTA-P-RGD .

Other Non-Primate Mammals

[PubMed]

No references are currently available.

Non-Human Primates

[PubMed]

No references are currently available.

Human Studies

[PubMed]

No references are currently available.

References

1. Shi J. et al. *Evaluation of In-Labeled Cyclic RGD Peptides: Effects of Peptide and Linker Multiplicity on Their Tumor Uptake, Excretion Kinetics and Metabolic Stability*. . *Theranostics*. 2011;1:322–40. PubMed PMID: 21850213.
2. Dijkgraaf I., Beer A.J., Wester H.J. *Application of RGD-containing peptides as imaging probes for alphavbeta3 expression*. . *Front Biosci*. 2009;14:887–99. PubMed PMID: 19273106.
3. Gaertner, F.C., M. Schwaiger, and A.J. Beer, *Molecular imaging of avb3 expression in cancer patients*. *Q J Nucl Med Mol Imaging*, 2010

4. Lu, X. and R.F. Wang, *A Concise Review of Current Radiopharmaceuticals in Tumor Angiogenesis Imaging*. Curr Pharm Des, 2012
5. Shi J.et al. *Impact of bifunctional chelators on biological properties of ¹¹¹In-labeled cyclic peptide RGD dimers*. . Amino Acids. 2011;41(5):1059–70. PubMed PMID: 20052508.
6. Liu S. *Radiolabeled cyclic RGD peptides as integrin $\alpha(v)\beta(3)$ -targeted radiotracers: maximizing binding affinity via bivalency*. . Bioconjug Chem. 2009;20(12):2199–213. PubMed PMID: 19719118.
7. Li Z.B.et al. *(⁶⁴Cu)-labeled tetrameric and octameric RGD peptides for small-animal PET of tumor $\alpha(v)\beta(3)$ integrin expression*. . J Nucl Med. 2007;48(7):1162–71. PubMed PMID: 17574975.
8. Poethko T.et al. *Chemoselective pre-conjugate radiohalogenation of unprotected mono- and multimeric peptides via oxime formation*. . Radiochim Acta. 2004;92:317–328.
9. Chakraborty S.et al. *Evaluation of ¹¹¹In-labeled cyclic RGD peptides: tetrameric not tetravalent*. . Bioconjug Chem. 2010;21(5):969–78. PubMed PMID: 20387808.
10. Shi J.et al. *Improving tumor uptake and pharmacokinetics of (⁶⁴Cu)-labeled cyclic RGD peptide dimers with Gly(3) and PEG(4) linkers*. . Bioconjug Chem. 2009;20(4):750–9. PubMed PMID: 19320477.
11. Liu Z.et al. *(⁶⁸Ga)-labeled cyclic RGD dimers with Gly3 and PEG4 linkers: promising agents for tumor integrin $\alpha(v)\beta(3)$ PET imaging*. . Eur J Nucl Med Mol Imaging. 2009;36(6):947–57. PubMed PMID: 19159928.
12. Shi J.et al. *Improving tumor uptake and excretion kinetics of ^{99m}Tc-labeled cyclic arginine-glycine-aspartic (RGD) dimers with triglycine linkers*. . J Med Chem. 2008;51(24):7980–90. PubMed PMID: 19049428.